Astrophysical reaction rates for ^{58,60}Ni(n,γ) from new neutron capture cross section measurements

K. H. Guber,[1,*] H. Derrien,[1] L. C. Leal,[1] G. Arbanas,[1] D. Wiarda,[1] P. E. Koehler,[2] and J. A. Harvey[2]
[1]*Nuclear Science and Technology Division, Oak Ridge National Laboratory, Oak Ridge, Tennessee 37831, USA*
[2]*Physics Division, Oak Ridge National Laboratory, Oak Ridge, Tennessee 37831, USA*
(Received 4 August 2010; revised manuscript received 22 September 2010; published 19 November 2010)

New neutron capture cross sections of ^{58,60}Ni were measured in the energy range from 100 eV to 600 keV using the Oak Ridge Electron Linear Accelerator. The combination of these new neutron capture data with previous transmission data allowed a resonance analysis up to 900 keV using *R*-matrix theory. The theoretically determined direct capture cross sections were included in the analyses. From these resonance parameters and the direct capture contribution, new (n,γ) astrophysical reaction rates were determined over the entire energy range needed by the latest stellar models describing the so-called weak *s* process.

DOI: 10.1103/PhysRevC.82.057601 PACS number(s): 25.40.Lw, 26.20.Kn, 27.40.+z, 27.50.+e

New improved neutron capture cross section measurements for ^{58,60}Ni were made in response to the Nuclear Criticality Safety Program (NCSP). Nickel, in addition to being a constituent in stainless steel and many other alloys, is one of the most abundant heavier elements in the universe. While performing critical benchmark calculations, deficiencies were identified for the nickel evaluations found in nuclear data libraries such as ENDF/B-VII [1] and JENDL-3.3 [2]. Many of the evaluations relied on experiments with known deficiencies, such as poor time-of-flight (TOF) resolution, and because of computer storage limitations, the description of some experimental neutron cross-section data in the neutron energy range above several tens of keV is crude. Consequently, the number of data points may not describe the resonances accurately enough to apply certain corrections, such as self-shielding, multiple scattering, or Doppler broadening of individual resonances. This impacts not only the cross section in the resolved resonance region but also the unresolved resonance region and could lead to problems in the correct processing of data from data libraries and possibly to erroneous Maxwellian average cross sections (MACS). These cross sections are also input parameters for models that describe nucleosynthesis in asymptotic giant branch stars via a chain of neutron capture reactions and β decays called the *s* process. From the astrophysical point of view, the nickel isotopes are very interesting because they are at the beginning of the *s*-process path. A recent study of the weak *s*-process component revealed that nuclides with smaller MACS act as bottlenecks and cause significant propagation effects of the *s*-process abundances calculated with stellar models for massive stars [3]. Also, because ^{58}Ni is very abundant [4] it is considered one of the most important seed nuclei for the weak component of the *s* process.

The ENDF/B-VII resonance evaluations for ^{58,60}Ni are mainly based on the experimental work of Refs. [5,6]. Our previous measurements (see, e.g., [7–11]) revealed that sample-dependent backgrounds sometimes were underestimated in prior experiments made with C_6F_6 detectors for nuclides, such as ^{58,60}Ni having resonances with large Γ_n/Γ_γ ratios. As shown in Fig. 1, our new data show several resonances for which this background was underestimated in previous experiments. Also because the (n,γ) measurements were performed with rather thick samples, corrections in the resonance analysis had to be applied for self-shielding and multiple scattering using analysis codes like SAMMY [12]. This required accurate neutron widths, which were determined by including high-resolution transmission data from Refs. [5,6,13] in the analysis. Over the years significant progress has been made and confidence gained in these corrections applied by the codes.

The experiments were performed using the Oak Ridge Electron Linear Accelerator (ORELA) [14], which is a high-intensity white neutron source with excellent timing resolution in the keV neutron energy range. Over the past 30 years ORELA has served as an excellent neutron source for many cross-section experiments. The neutron energy was determined using the TOF technique. ORELA operated with a repetition rate of 525 Hz, 8-ns pulse width, and an average power of 6 kW. The neutron capture experiments were performed using two isotopically enriched rectangular metallic nickel samples. These were mounted in the sample holder, so that they were completely illuminated by the 2.7×5.2 cm neutron beam. The sample characteristics are compiled in Table I. The measurements were performed using the pulse-height-weighting technique [15] with a pair of C_6D_6 scintillation detectors located at a distance of 40.12 m from the neutron production target. The energy-dependent neutron flux was measured simultaneously by a 0.5-mm-thick ^{6}Li-loaded glass scintillation detector which was positioned 43 cm before the sample. Additional measurements were performed with no sample and a carbon sample to determine the smoothly varying backgrounds. A ^{10}B overlap filter was placed into the neutron beam to eliminate low-energy neutrons from the preceding pulse and a lead filter to reduce the γ flash; these filters were located at a distance of 5 m from the neutron target. Normalization of the cross section was accomplished using a gold sample and the saturated resonance technique [16]. The original capture system [15] has undergone major changes compared to the previous nickel

*Corresponding author: guberkh@ornl.gov

 ©2010 The American Physical Society

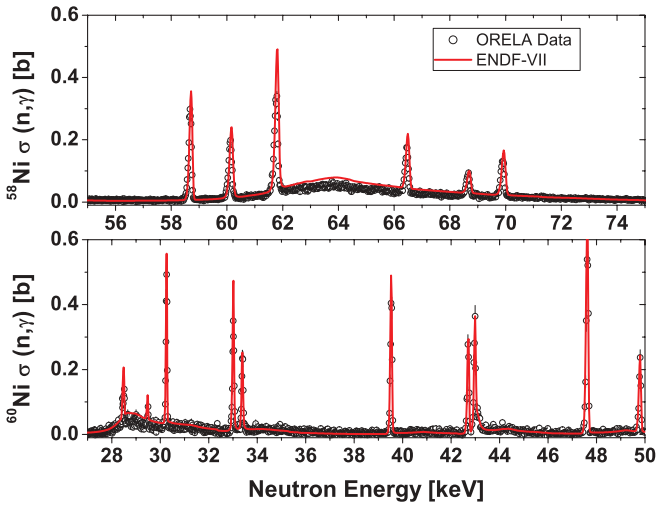

FIG. 1. (Color online) Representative comparisons of our Ni capture data (error bars are smaller than the symbols) to SAMMY calculations (solid curve) using the ENDF/B-VII resonance parameters. Corrections due to experimental effects, such as sample multiple scattering and self-shielding, are included in the calculation. This plot illustrates, for example, that the background due to sample scattered neutrons was underestimated in prior measurements, resulting in a capture area too large for the 62.3-keV resonance in ^{58}Ni.

neutron capture experiments [5,6]. The changes described in Ref. [7] resulted in a significantly reduced sensitivity to sample scattered neutrons [8] and have also contributed to a simplification, improved reliability and a better method for calculating the pulse-height-weighting function. The latter was calculated using the Monte Carlo code MCNP [17], including all sample-related and experimental effects such as γ-ray attenuation in the sample and resolution broadening. As demonstrated in cases of the (n,γ) cross-section measurements for ^{136,134}Ba, ^{88}Sr, ^{142,144}Nd, ^{35,37}Cl, and natural silicon [7–11], the experimental apparatus is well suited for measuring small neutron capture cross sections, such as those of the nickel isotopes.

As for many nuclides with very small (n,γ) cross sections, the direct capture (DC) component can be a sizable part of the reaction rates. The low-energy direct-semidirect (DSD) capture of s-wave neutrons on ^{58,60}Ni was computed using the code CUPIDO [18]. The spectroscopic factors for this computation were taken from Ref. [19], whereas the potential for scattering states was taken to be the real part of the Koning-Delaroche global optical potential [20]. For low-energy neutrons, the DC occurs mainly through the s-wave channel via an electric dipole ($E1$) transition to a bound state of the (target + neutron) composite nucleus. Selection rules for $E1$ capture of s-wave neutrons restrict the angular momentum of the bound states to $l = 1$. The potential used for the calculation of $l = 1$ bound states was taken from Ref. [21]. d-wave capture to $l = 1$ bound states was included in the calculations but was found to be small. The DSD calculations were performed from thermal energy to 2.5 MeV. $E1$ direct capture of p-wave neutrons into $l = 0$ bound states was assumed to be negligible because $l = 0$ bound states lie higher in energy, thus yielding less energetic γ rays, and hence a small cross section, as the capture cross section is proportional to the third power of γ-ray energy.

TABLE I. Isotopic enrichment and dimensions for the nickel samples.

Isotope	Enrichment (%)	Weight (g)	Height (cm)	Width (cm)	Thickness	
					(cm)	(atom/barn)
^{58}Ni	99.9	45.4307	5.038	2.577	0.413	0.036 35
^{60}Ni[a]	99.6	48.5728	5.161	2.628	0.406	0.035 98

[a]0.34% ^{58}Ni, 0.02% ^{61}Ni, 0.03% ^{62}Ni.

A significant destructive interference between the direct and the semidirect capture components caused the DSD capture to be about one-half of the pure direct capture, thus demonstrating the significance of including the semidirect component for these nuclides. This destructive interference partially explains why our DSD capture is substantially lower than the thermal DC cross section reported in Ref. [19]. Several bound-state levels in Ref. [19] were listed as either spin 1/2 or 3/2, and it was found that the choice of the spin can affect the computed capture by as much as 10%. An additional error factor has been introduced to account for the uncertainties inherent in the spectroscopic factors, which were estimated to be about 20%. The thermal DSD capture cross sections on ^{58}Ni and ^{60}Ni were computed to be 1.5 and 0.5 b, respectively, with ~25% relative uncertainty.

The transmission and new capture data were analyzed in the resolved resonance region using the multilevel $\mathcal{R}$-matrix code SAMMY. The nickel data were fitted in the energy range from 0.0254 eV to ~900 keV, where 490 resonances were fitted for ^{58}Ni and 471 for ^{60}Ni. This is slightly more than reported in Ref. [6] for ^{58}Ni. But for ^{60}Ni we were able to extend the resolved range by almost a factor of 2 compared to Ref. [5] due to our high resolution capture data and the high resolution transmission from Ref. [13]. Details about the resonance analysis and evaluation, including covariances, will be published separately [22].

We calculated the MACS for ^{58,60}Ni(n,γ) due to our resonance parameters using standard techniques [23]. The DC contributions were added to the resonance contributions to obtain the total MACS. The new rates for ^{58}Ni and ^{60}Ni are reported in separate columns for the resonance and the DC parts and compared to the most recent evaluations in Tables II and III. The reported uncertainties of our data, which include statistical and experimental systematic uncertainties as well as 25% uncertainty in the DC calculations, were obtained from the new evaluations [22]. A closer examination of our uncertainties for the resonance part reveals that the 3.5% systematic uncertainty from the normalization is the dominating factor in the Maxwellian average reaction rate uncertainties.

From our new data we find lower MACS values (resonance and DC part) for ^{58}Ni compared to evaluations [23–26], ranging from 10% to 20% for $kT = 30$ keV. Over the entire temperature range the reported MACS are smaller than the

TABLE II. MACS for ^{58}Ni compared to the most recent evaluations [23–26]. Uncertainties are reported as found in the evaluations.

kT (keV)	Resonance part	DC part	[23] (mb)	[24]	[25]	[26]
5	35.50 ± 1.24	3.49 ± 0.87	45.1	39.8	40.42	38.3
8	45.05 ± 1.58	2.74 ± 0.68				
10	45.95 ± 1.61	2.44 ± 0.61	58.3	52.0	52.08	50.1
15	42.93 ± 1.50	1.97 ± 0.49	54.6	49.9	49.76	48.1
20	38.82 ± 1.36	1.69 ± 0.42	49.7	46.2	45.97	44.5
25	35.38 ± 1.24	1.50 ± 0.38	45.5	42.9	42.66	41.3
30	32.67 ± 1.14	1.36 ± 0.34	42.3 ± 2.8	41.0 ± 2.0	40.01	38.7 ± 1.5
35	30.51 ± 1.07	1.25 ± 0.31			37.88	
40	28.75 ± 1.01	1.16 ± 0.29	37.7	36.3	36.12	35.0
50	26.03 ± 0.91	1.03 ± 0.26	34.5	33.5	33.34	30.1
60	23.97 ± 0.84	0.93 ± 0.23	32.2	31.3		
70	22.33 ± 0.78	0.85 ± 0.21			29.35	
80	20.98 ± 0.73	0.79 ± 0.20	28.9	28.0		27.0
100	18.87 ± 0.66	0.70 ± 0.17	26.8	25.3	25.23	24.4

evaluations and show a different temperature dependence. In a recent experiment the MACS for ^{58}Ni was determined by activation and accelerator mass spectrometry [27]. This completely different approach in determining the MACS resulted in a much lower value, 27.2 ± 2.1 for kT = 25 keV, compared to previous experiments and evaluations. This is a difference of almost 30%, compared to our value at kT = 25 keV, well outside the reported uncertainties, and cannot be explained by experimental effects such as neutron sensitivity of the experimental setup. The two strongest s-wave resonances in ^{58}Ni at neutron energies of 15.07 and 62.26 keV contribute almost 5 mb to the MACS at this temperature. Even a reduction of these contributions by 50% due to an assumed neutron sensitivity of the experimental setup cannot make up the difference to the value of Ref. [27].

Our MACS for ^{60}Ni are lower than the evaluation of Ref. [24]; we find a 10% smaller cross section for kT = 30 keV. Consequently our values are also lower than Ref. [26] which are normalized to the 30-keV value of Ref. [24]. On the other hand, the evaluation of Ref. [23] is almost 10% lower at kT = 5 keV which uses ENDF/B-VII resonance parameters, is 4% lower at low kT and, due to the different energy dependence, crosses our data at 20 keV. In the relatively new cross section determination of ^{60}Ni [28] an almost 10% lower MACS compared to ours is found over the entire energy range, but the results are within the reported uncertainties if only the resonance part is compared. To better emphasize the differences in the reaction rates, we plotted the MACS of the evaluations relative to our MACS. These ratios are shown in Fig. 2 for ^{58}Ni and Fig. 3 for ^{60}Ni, respectively.

In general, our new ^{58,60}Ni(n,γ) MACS are smaller than previous results at weak s-process temperatures, which could impact estimates of the s-process nucleosynthesis in massive stars. Those stellar models operate at different neutron pulse

TABLE III. MACS for ^{60}Ni compared to the most recent evaluations [23–26]. Uncertainties are reported as found in the evaluations.

kT (keV)	Resonance part	DC part	[23] (mb)	[24]	[25]	[26]
5	63.28 ± 2.21	1.26 ± 0.32	59.06	79	62.12	69.9± 4.9
8	60.21 ± 2.11	1.01 ± 0.25				66.5± 4.6
10	54.86 ± 1.92	0.91 ± 0.23	54.3	70	54.81	60.8 ± 4.1
15	43.09 ± 1.51	0.76 ± 0.19	43.06	57	43.98	48.1± 3.0
20	35.23 ± 1.23	0.66 ± 0.17	35.33	46	36.61	39.6± 2.3
25	30.05 ± 1.05	0.59 ± 0.15	30.21	41	31.68	33.8 ± 1.8
30	26.47 ± 0.93	0.54 ± 0.13	26.7 ± 1.4	30 ± 3.0	28.26	29.9± 0.7
35	23.87 ± 0.84	0.50 ± 0.12	24.18		25.78	
40	21.92 ± 0.77	0.46 ± 0.12	22.29	28	23.89	24.8 ± 1.2
50	19.15 ± 0.67	0.41 ± 0.10	19.6	27	21.21	21.7 ± 1.1
60	17.29 ± 0.61	0.37 ± 0.09	17.89	24		19.5 ± 1.0
70	15.96 ± 0.56	0.34 ± 0.08			18.02	
80	14.96 ± 0.52	0.32 ± 0.08	15.73	21		16.7 ± 0.8
100	13.53 ± 0.47	0.28 ± 0.07	14.47	20	15.4	14.7 ± 0.7

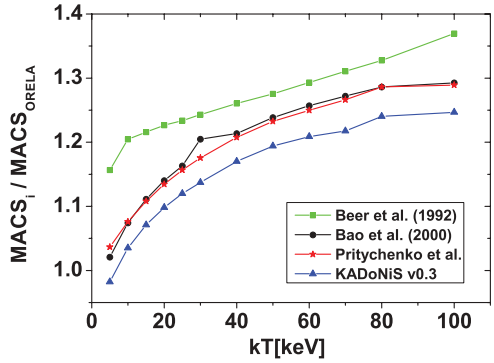

FIG. 2. (Color online) ^{58}Ni MACS from the evaluations of Refs. [23–26] relative to our work.

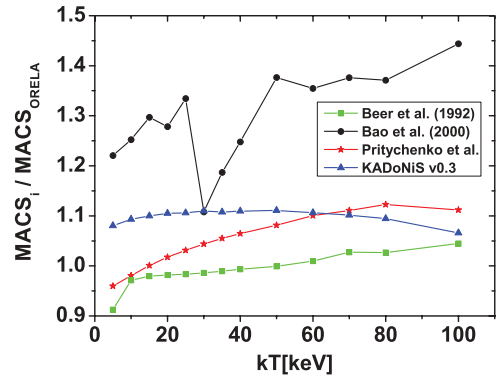

FIG. 3. (Color online) ^{60}Ni MACS from the evaluations of Refs. [23–26] relative to our work.

temperatures $kT = 25$ and 90 keV, compared to models of the main component ($kT = 8$ and 23 keV).

We would like to acknowledge C. Ausmus, D. Brasher, J. White, and T. Bigelow who kept ORELA smoothly running. The enriched metallic capture samples were prepared by C. Ausmus. ORNL is managed by UT-Battelle, LLC, for the US Department of Energy under Contract No. DE-AC05-00OR22725. The work that is presented in this paper was sponsored by the US Department of Energy's Nuclear Criticality Safety Program and the Office of Science.

[1] M. B. Chadwick *et al.*, Nucl. Data Sheets **107**, 2931 (2006).
[2] T. Nakagawa *et al.*, J. Nucl. Sci. Technol. **32**, 1259 (1995).
[3] M. Heil, F. Käppeler, E. Uberseder, R. Gallino, and M. Pignatari, Phys. Rev. C **77**, 015808 (2008).
[4] E. Anders and N. Grevesse, Geochim. Cosmochim. Acta **53**, 197 (1989).
[5] C. M. Perey, J. A. Harvey, R. L. Macklin, F. G. Perey, and R. R. Winters, Phys. Rev. C **27**, 2556 (1983).
[6] C. M. Perey, F. G. Perey, J. A. Harvey, N. W. Hill, N. M. Larson, R. L. Macklin, and D. C. Larson, Phys. Rev. C **47**, 1143 (1993).
[7] P. E. Koehler, R. R. Spencer, R. R. Winters, K. H. Guber, J. A. Harvey, N. W. Hill, and M. S. Smith, Phys. Rev. C **54**, 1463 (1996).
[8] P. E. Koehler *et al.*, Phys. Rev. C **62**, 055803 (2000).
[9] K. H. Guber, R. R. Spencer, P. E. Koehler, and R. R. Winters, Phys. Rev. Lett. **78**, 2704 (1997).
[10] R. O. Sayer, K. H. Guber, L. C. Leal, N. M. Larson, and T. Rauscher, Phys. Rev. C **73**, 044603 (2006).
[11] K. H. Guber, P. E. Koehler, H. Derrien, T. E. Valentine, L. C. Leal, R. O. Sayer, and T. Rauscher, Phys. Rev. C **67**, 062802(R) (2003).
[12] N. M. Larson, Oak Ridge National Laboratory Technical Report No. ORNL/TM-9179/R8, 2008 (unpublished).
[13] A. Brusegan, G. Rohr, R. Shelly, E. Macavero, C. Van der Vorst, F. Poortmans, I. Mewissen, and G. Vanpraet, in *Proceedings of the International Conference on Nuclear Data for Science and Technology*, *Gatlinburg, Tennessee*, *1994*, edited by J. K. Dickens (American Nuclear Society, La Grange Park, IL, 1994), Order No. 700205, p. 224.
[14] K. H. Guber, D. C. Larson, P. E. Koehler, R. R. Spencer, S. Raman, J. A. Harvey, N. W. Hill, T. A. Lewis, and R. R. Winters, in *Proceedings of the International Conference on Nuclear Data for Science and Technology*, edited by G. Reffo, A. Ventura, and C. Grandi, Italian Physical Society Conference Proceedings Vol. 59 (Italian Physical Society, Bologna, Italy, 1998), Part I, p. 559.
[15] R. L. Macklin and B. J. Allen, Nucl. Instrum. Methods **91**, 565 (1971).
[16] R. L. Macklin, J. Halperin, and R. R. Winters, Nucl. Instrum. Methods **164**, 213 (1979).
[17] J. F. Briesmeister, Ed., "MCNP – A General Monte Carlo N-Particle Transport Code—Version 4C", Los Alamos National Laboratory Report, LA-13709-M.
[18] W. E. Parker *et al.*, Phys. Rev. C **52**, 252 (1995).
[19] S. Raman, X. Ouyang, M. A. Islam, J. W. Starner, E. T. Journey, J. E. Lynn, and G. Martinez-Pinedo, Phys. Rev. C **70**, 044318 (2004).
[20] A. J. Koning and J. P. Delaroche, Nucl. Phys. A **713**, 231 (2003).
[21] K. Bear and P. E. Hodgson, J. Phys. G **4**, L287 (1978).
[22] H. Derrien, to be published as Oak Ridge National Laboratory Technical Report (unpublished).
[23] H. Beer, F. Voss, and R. R. Winters, Astrophys. J. Suppl. Ser. **80**, 403 (1992).
[24] Z. Y. Bao, H. Beer, F. Käppeler, F. Voss, K. Wisshak, and T. Rauscher, At. Data Nucl. Data Tables **76**, 70 (2000).
[25] B. Pritychenko, S. F. Mughaghab, and A. A. Sonzongi, At. Data Nucl. Data Tables **96**, 645 (2010).
[26] I. Dillmann, R. Plag, F. Käppeler, and T. Rauscher, KADoNiS, Version 0.3 [http://www.kadonis.org/].
[27] G. Rugel, I. Dillmann, T. Faestermann, M. Heil, F. Käppeler, K. Knie, G. Korschniek, W. Kutschera, M. Poutivtsev, and A. Wallner, Nucl. Instrum. Methods Phys. Res. B **259**, 683 (2007).
[28] F. Corvi, G. Fioni, F. Gunsing, P. Mutti, and L. Zanini, Nucl. Phys. A **697**, 581 (2002).